Model of the Optical Emission of a Driven Semiconductor Quantum Dot: Phonon-Enhanced Coherent Scattering and Off-Resonant Sideband Narrowing

Dara P. S. McCutcheon[1,2,*] and Ahsan Nazir[2,†]

[1]*Departamento de Física, FCEyN, UBA and IFIBA, Conicet, Pabellón I, Ciudad Universitaria, 1428 Buenos Aires, Argentina*
[2]*Blackett Laboratory, Imperial College London, London SW7 2AZ, United Kingdom*

(Received 12 September 2012; published 21 May 2013)

We study the crucial role played by the solid-state environment in determining the photon emission characteristics of a driven quantum dot. For resonant driving, we predict a phonon enhancement of the coherently emitted radiation field with increasing driving strength, in stark contrast to the conventional expectation of a rapidly decreasing fraction of coherent emission with stronger driving. This surprising behavior results from thermalization of the dot with respect to the phonon bath and leads to a nonstandard regime of resonance fluorescence in which significant coherent scattering and the Mollow triplet coexist. Off resonance, we show that despite the phonon influence, narrowing of dot spectral sideband widths can occur in certain regimes, consistent with an experimental trend.

DOI: 10.1103/PhysRevLett.110.217401 PACS numbers: 78.67.Hc, 71.38.−k, 78.47.−p

As described by Mollow, the spectrum of light scattered from a resonantly driven two-level system (TLS) depends crucially on the relative size of the laser driving strength to the TLS radiative decay rate [1]. For weak driving, the light is predominately coherently (or elastically) scattered, resulting in a single (delta function) peak in the emission spectrum at the laser frequency. At larger driving strengths, however, coherent scattering is strongly suppressed, and the emission becomes dominated by incoherent (inelastic) scattering from the TLS-laser dressed states [2]. This results in a triple-peak structure in the spectrum, known as the Mollow triplet.

Whereas these fundamental predictions have long been confirmed in the traditional quantum optical setting of driven atoms [3], more recently interest has turned to their observation in solid-state TLSs (artificial atoms) such as semiconductor quantum dots (QDs) [4–10], single molecules [11], and superconducting circuits [12]. In the particular case of QDs, many of the archetypal features of atomic quantum optics have now been demonstrated, such as resonance fluorescence [4–10], coherent population oscillations [7,13–15], photon antibunching [16,17], and two-photon interference [18–20]. Aside from being of fundamental interest, these observations also pave the way towards using QDs as efficient single-photon sources [21–24] and for other quantum technologies [25].

Thus, under appropriate conditions, the emission properties of a driven QD can bear close resemblance to the more idealized case of a driven atom in free space. QDs are, nevertheless, unavoidably coupled to their surrounding solid-state environments. For coherently driven (ground state) excitonic transitions in typical arsenide QDs, coupling to acoustic phonons has been demonstrated to dominate the QD-environment interaction [14,15], leading to the appearance of an excitation-induced dephasing contribution with a rate that varies with the square of the Rabi frequency (dot-laser coupling strength) [9,14,15,26]. This driving dependence is theoretically understood as resulting from phonons that induce transitions between the dressed states of the QD at the Rabi energy [26–29], making it the relevant energy scale in the three-dimensional phonon environment.

We shall show here that such transitions can lead to QD emission characteristics that deviate fundamentally from the well-established quantum optical behavior outlined above. Specifically, we investigate the competition between photon emission and phonon effects in both the coherent and incoherent scattering properties of a driven QD [30–34]. As our main result, we show that in the presence of phonon coupling the coherent contribution to the QD resonance fluorescence can actually *increase* with driving strength, in a striking departure from the conventional behavior in the atomic case. This stems from phonon transitions driving thermalization among the dot dressed states in the system steady state, an effect that arises naturally in our microscopic model of the phonon bath but cannot be captured by a simplified treatment in terms of a phenomenological pure dephasing process. As the total scattered light is limited by the photon emission rate, a corresponding *decrease* of incoherent emission occurs in the same regime, a trend which a standard quantum optics treatment is again unable to reproduce. We also find that, in an appropriate parameter regime, our model predicts a narrowing of the Mollow sidebands as the QD-laser detuning is increased, consistent with recent experimental observations [9].

We model the QD as a TLS with ground state $|0\rangle$ and excited (single exciton) state $|X\rangle$, split by an energy $\hbar\omega_0$. The dot is driven by a laser of frequency ω_l, with Rabi frequency Ω, and coupled to two separate harmonic oscillator baths to account for both phonon interactions and spontaneous emission into the radiation field. In a frame rotating at frequency ω_l and after a rotating wave approximation on the driving term, our Hamiltonian takes the form ($\hbar = 1$)

$$H = \nu|X\rangle\langle X| + \frac{\Omega}{2}\sigma_x + \sum_{\mathbf{k}}\omega_{\mathbf{k}} b_{\mathbf{k}}^\dagger b_{\mathbf{k}} + \sum_{\mathbf{q}}\eta_{\mathbf{q}} a_{\mathbf{q}}^\dagger a_{\mathbf{q}} + |X\rangle\langle X|\sum_{\mathbf{k}} g_{\mathbf{k}}(b_{\mathbf{k}}^\dagger + b_{\mathbf{k}}) + \sum_{\mathbf{q}}(h_{\mathbf{q}} a_{\mathbf{q}} e^{i\omega_l t}\sigma_+ + \text{H.c.}),$$

where $\nu = \omega_0 - \omega_l$ is the QD-laser detuning, $\sigma_+ = |X\rangle\langle 0|$ ($\sigma_- = \sigma_+^\dagger$), $\sigma_x = \sigma_+ + \sigma_-$, and H.c. denotes the Hermitian conjugate. The phonon bath is represented by creation (annihilation) operators $b_{\mathbf{k}}^\dagger$ ($b_{\mathbf{k}}$) for modes with frequency $\omega_{\mathbf{k}}$, which couple to the QD with strength $g_{\mathbf{k}}$. The photon bath is similarly defined, with operators $a_{\mathbf{q}}^\dagger$ ($a_{\mathbf{q}}$), frequencies $\eta_{\mathbf{q}}$, and couplings $h_{\mathbf{q}}$.

Obtaining an equation of motion for the QD dynamics can be achieved in various ways, such as through master equations of weak coupling [26,27], polaron [29–31,35], and variational type [36] as well as by several numerical methods [28,37,38]. For our purposes, master equations are particularly attractive since, with use of the quantum regression theorem [2], they can readily be applied to investigate emitted field correlation properties [30,31]. Thus, we opt here to extend the variational approach of Ref. [36] to include the photon bath, in order to calculate field correlations, as it is limited neither to weak phonon coupling nor to the small driving limit of polaron theory.

To the full Hamiltonian, we apply a QD-state-dependent phonon displacement transformation $H_V = e^V H e^{-V}$, with $V = |X\rangle\langle X|\sum_{\mathbf{k}}(F(\omega_{\mathbf{k}})/\omega_{\mathbf{k}})(g_{\mathbf{k}} b_{\mathbf{k}}^\dagger - g_{\mathbf{k}}^* b_{\mathbf{k}})$. The magnitudes of the displacements are chosen to minimize a free energy bound on the resulting interaction terms in H_V [39]. Applying the time-convolutionless projection operator technique to second order in the transformed frame, we find a master equation of the form (Supplemental Material [40])

$$\dot\rho_V = -\frac{i}{2}[\epsilon\sigma_z + \Omega_r\sigma_x, \rho_V] + \mathcal{K}_{\text{ph}}(\rho_V) + \mathcal{K}_{\text{sp}}(\rho_V). \quad (1)$$

Here, $\rho_V = \text{Tr}_B(e^V \chi e^{-V})$, with χ the complete density operator, is the reduced state of the QD TLS in the variational frame, $\epsilon = \nu + \int_0^\infty J_{\text{ph}}(\omega)\omega^{-1}F(\omega)[F(\omega) - 2]d\omega$ and $\Omega_r = \Omega\exp[-(1/2)\int_0^\infty J_{\text{ph}}(\omega)\omega^{-2}F(\omega)^2\coth(\beta\omega/2)d\omega]$, with temperature $T = 1/(k_B\beta)$, are the phonon renormalized detuning and Rabi frequency, respectively, whereas $\mathcal{K}_{\text{sp}}(\rho_V) = \Gamma_1(\sigma_-\rho_V\sigma_+ - (1/2)\{\sigma_+\sigma_-, \rho_V\})$ accounts for spontaneous emission. The variational factor $F(\omega) = [1 - (\epsilon/\xi)\tanh(\beta\xi/2)][1 - (\epsilon/\xi)\tanh(\beta\xi/2)(1 - (\Omega_r^2/2\epsilon\omega)\coth(\beta\omega/2))]^{-1}$, with $\xi = \sqrt{\epsilon^2 + \Omega^2}$, is bounded between zero (for no transformation) and unity (for the polaron transformation), and the QD-phonon spectral density is usually parametrized by $J_{\text{ph}}(\omega) = \alpha\omega^3\exp[-(\omega/\omega_c)^2]$ for coupling to acoustic phonons [14,15]. The term $\mathcal{K}_{\text{ph}}(\rho_V)$, defined in full in the Supplemental Material [40], contains all phonon effects other than those included in ϵ and Ω_r, representing the various processes induced by phonon interactions, such as pure dephasing, phonon emission, and absorption.

We characterize the QD photon emission through the steady-state first-order field correlation $g^{(1)}(\tau) = \lim_{t\to\infty}\langle\sigma_+(t)\sigma_-(t+\tau)\rangle$. The coherent contribution, defined as $g_{\text{coh}}^{(1)} = \lim_{\tau\to\infty} g^{(1)}(\tau)$, is related to the off-diagonal elements of the QD density operator in the steady state, $g_{\text{coh}}^{(1)} = |\rho_{0X}|^2$, and is thus a direct consequence of nonvanishing QD coherence. The incoherent contribution is then given by $g_{\text{inc}}^{(1)}(\tau) = g^{(1)}(\tau) - g_{\text{coh}}^{(1)}$, which determines the incoherent QD emission spectrum via $S_{\text{inc}}(\omega) \propto (1/\pi)\,\text{Re}[\int_0^\infty e^{i(\omega-\omega_l)\tau} g_{\text{inc}}^{(1)}(\tau)d\tau]$.

Enhanced coherent scattering.—We begin our analysis by investigating the emission properties of the QD when driven on resonance with the polaron-shifted transition frequency [$\epsilon_{F(\omega)\to 1} = 0$]. We are interested in examining the detailed effects induced by the coupling to phonons as the driving strength is varied. In particular, we would like to explore deviations from the phenomenological—though often employed and standard in quantum optics [2]—treatment of environmental interactions (beyond radiative decay) as giving rise simply to sources of pure dephasing. In fact, we find that the full phonon influence can *only* be represented by a pure dephasing form (Supplemental Material [40]), $\mathcal{K}_{\text{ph}}(\rho_V) \approx (1/2)\gamma_{\text{PD}}(\sigma_z\rho_V\sigma_z - \rho_V)$, for weak resonant driving strengths satisfying $\Omega < k_B T < \omega_c$, consistent with experimental results in this regime [5,7,9,14,15]. Here, the rate reduces to that given by polaron theory [29,30], $\gamma_{\text{PD}} = (\Omega_r/2)^2\int_{-\infty}^\infty\cos(\Omega_r s)(e^{\phi(s)} - e^{-\phi(s)})ds$, where $\phi(s) = \int_0^\infty J(\omega)\omega^{-2}(\cos(\omega s)\coth(\beta\omega/2) - i\sin(\omega s))d\omega$, while $F(\omega)\to 1$ in Eq. (1). Within this limit, we can derive an analytic expression for $g^{(1)}(\tau)$, giving

$$g_{\text{inc}}^{(1)}(\tau) = \frac{\Omega_r^2}{2\Omega_r^2 + 2\Gamma_1\Gamma_2}\left[\frac{1}{2}e^{-\Gamma_2\tau} + e^{-1/2(\Gamma_1+\Gamma_2)\tau}(N\cos(\zeta\tau) - M\sin(\zeta\tau))\right], \quad (2)$$

where $\Gamma_2 = (1/2)\Gamma_1 + \gamma_{\text{PD}}$, $\zeta = \sqrt{\Omega_r^2 - (1/4)(\Gamma_1 - \Gamma_2)^2}$, $N = [\Omega_r^2 - \Gamma_1(\Gamma_1 - \Gamma_2)]/(2\Omega_r^2 + 2\Gamma_1\Gamma_2)$, and $M = [\Omega_r^2(\Gamma_2 - 3\Gamma_1) + \Gamma_1^3\Gamma_2^2(\Gamma_1^{-1} - \Gamma_2^{-1})^2]/[4\zeta(\Omega_r^2 + \Gamma_1\Gamma_2)]$, and

$$g_{\text{coh}}^{(1)} = \left(\frac{\Gamma_1\Omega_r}{2\Gamma_1\Gamma_2 + 2\Omega_r^2}\right)^2. \quad (3)$$

Note that in the pure dephasing model, $g_{\text{coh}}^{(1)} \to 0$ if Ω_r is allowed to become large, precisely as in the atomic case.

In fact, Eqs. (2) and (3) are essentially the standard atomic $g^{(1)}$ expressions when extended to include pure dephasing [5,7]. The only difference here is that we explicitly include a *driving-dependent* pure-dephasing rate

$\gamma_{\rm PD} \sim \Omega_r^2$ (for $\beta\Omega_r$, $\Omega_r/\omega_c \ll 1$) and that the driving is itself renormalized by phonons through Ω_r. While both of these features are important to approximate the full dynamics, neither will give rise to the kind of pronounced, phonon-induced deviations from standard atomic behavior in which we are interested.

To exemplify the breakdown of the pure-dephasing model, in Fig. 1 we plot $g^{(1)}(\tau)$ calculated using the full variational theory (solid blue curves) and calculated using Eqs. (2) and (3) (black dashed curves). As expected, for weaker driving, $\Omega < 0.1\ \mathrm{ps}^{-1}$, the pure dephasing model gives a good approximation to the full theory. Nevertheless, as the driving strength is increased, significant discrepancies soon become apparent. In particular, from the different long-time values approached when $\Omega \geq 0.33\,\mathrm{ps}^{-1}$, we conclude that the coherent contribution surprisingly becomes important in this regime and that this

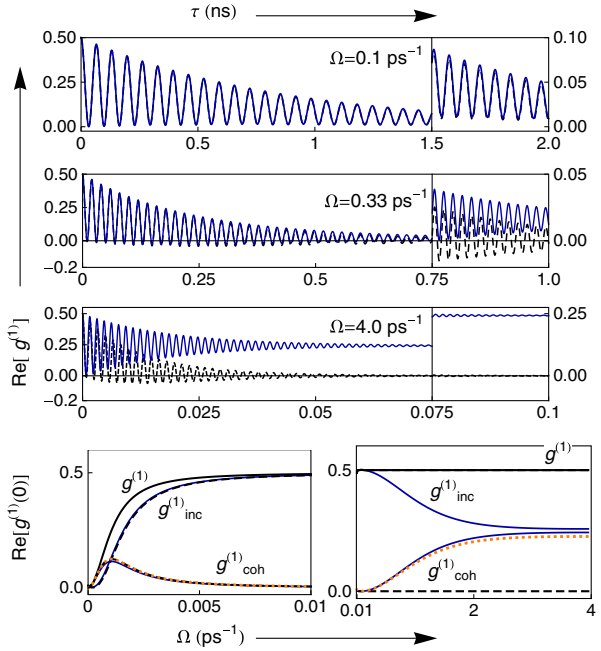

FIG. 1 (color online). Upper three plots: First-order field correlation function for various driving strengths, as indicated, calculated from the full variational theory (blue solid curves) and the pure dephasing approximation of Eqs. (2) and (3) (black dashed curves). The rightmost parts show enlargements of the long-time behavior. Lower plots: Coherent ($g^{(1)}_{\rm coh}$), incoherent ($g^{(1)}_{\rm inc}$), and total ($g^{(1)}$) scattering as a function of driving strength, calculated using the full (blue solid curves) and pure dephasing (black dashed curves) theories. The total scattering is indistinguishable on this scale between the two models. However, the left plot shows the only region where the pure dephasing model gives a non-negligible coherent contribution, close to the origin; i.e., in the pure dephasing case, all light is incoherently scattered in the right plot. Shown also is $g^{(1)}_{\rm coh}$ calculated from Eq. (4) (orange dotted curve). Parameters: $T_1 = 700$ ps, $\alpha = 0.027\ \mathrm{ps}^2$, $\omega_c = 2.2\ \mathrm{ps}^{-1}$, and $T = 4$ K.

feature is not captured by the pure dephasing approximation. Indeed, when $\Omega = 4\,\mathrm{ps}^{-1}$, the full phonon theory gives $g^{(1)}_{\rm coh} \sim 0.25$, in clear distinction to the pure dephasing case.

That Eqs. (2) and (3) cannot capture these effects signifies that above a driving strength of $\Omega \sim 0.1\ \mathrm{ps}^{-1}$ (for these realistic parameters), the field correlation properties of the QD emission fundamentally depart from the atomic case. At driving above saturation, photons mediate transitions between manifolds of the dot-laser dressed states, while phonons mediate transitions between dressed states in a single manifold. Hence, photon emission acts in this regime to completely suppress QD coherences in the steady state, whereas phonons drive thermalization among the dressed states, thus leading to QD steady states with non-negligible coherence. When phonon processes dominate over photon emission, as in the strong-driving regime, we then find that the level of coherent emission correspondingly grows. Though the pure dephasing model correctly captures the fact that phonon-induced damping remains driving dependent across the full parameter range, it fails here because it does not lead to the correct equilibration of the QD with the phonon bath. In this regard, it assumes a high temperature limit with respect to the driving strength, and thus the quantum nature of the environment is lost.

For resonant driving, we can (approximately) rectify this by the modification $\mathcal{K}_{\rm ph}(\rho_V) \approx (1/2)\gamma_{\rm PD}(\sigma_z\rho_V\sigma_z - \rho_V) + (i/4)\kappa[\sigma_y, \{\sigma_z, \rho_V\}]$, where $\kappa = (\Omega_r/2)^2 \int_{-\infty}^{\infty} \sin(\Omega_r s) \times (e^{\phi(s)} - e^{-\phi(s)})ds$, such that $\kappa/\gamma_{\rm PD} = \tanh(\beta\Omega_r/2)$. We now find

$$g^{(1)}_{\rm coh} \to G^{(1)}_{\rm coh} = \left(\frac{\Gamma_1\Omega_r}{2\Gamma_1\Gamma_2 + 2\Omega_r^2}\right)^2 + \left(\frac{\Omega_r\kappa/\Omega}{\Gamma_1 + 2\gamma_{\rm PD}}\right)^2, \quad (4)$$

where the first term is precisely the contribution in the strict pure-dephasing case [see Eq. (3)], which quickly becomes negligible for large Ω_r. Conversely, the second term, now arising due to equilibration with the quantum mechanical phonon bath, becomes important as Ω_r increases. To see this, we note that once Ω_r is large enough such that $\Gamma_1 \ll \gamma_{\rm PD}$, we can approximate $G^{(1)}_{\rm coh} \approx [\Omega_r \tanh(\beta\Omega_r/2)/2\Omega]^2$. In the upper three plots of Fig. 1, increasing the driving moves the QD from an effective high-temperature regime, where $\beta\Omega_r \ll 1$ and $G^{(1)}_{\rm coh} \approx 0$, to an effective low-temperature regime, where $\beta\Omega_r \gg 1$ and $G^{(1)}_{\rm coh} \approx (\Omega_r/2\Omega)^2$. These observations are borne out in the lower part of Fig. 1, where we plot the coherent, incoherent, and total scattering as a function of Ω. The lower left plot shows the region close to the origin, the only regime in which the pure dephasing model predicts a non-negligible level of coherent emission. From the lower right plot, we see also that as the total scattering is fixed at strong driving, the incoherent contribution decreases in our full phonon model as the coherent contribution increases. Again, this is not captured by the pure dephasing treatment. In fact, this represents a hitherto

unexplored regime of resonance fluorescence at strong driving, in which both significant coherent scattering and a well-defined Mollow triplet can coexist.

QD resonance fluorescence experiments are usually performed at Rabi frequencies up to around 25 GHz ($\Omega = 0.16$ ps^{-1}), at which point the coherent fraction is of order 1% from our full phonon model, compared to 0.01% in the pure dephasing model (for the parameters of Fig. 1). Upon a fourfold increase of Ω, around 15% of the light is then coherently scattered in the full model, compared to less than 0.0003% in the pure dephasing case. Upon a reduction of the temperature to 2 K, the coherent fraction could be increased to about 35% at this driving strength.

Spectrum.—We now turn our attention to the QD emission spectrum, concentrating on cases where the incoherent contribution dominates (i.e., relatively weak driving), and Eq. (2) is thus approximately valid on resonance. From a Fourier transform of Eq. (2), we find that the resonant Mollow sideband widths are determined by $\Gamma_1 + \Gamma_2 = (3/2)\Gamma_1 + \gamma_{\rm PD}$, with approximate positions $\pm\Omega_r$. We therefore expect a systematic broadening and splitting with increasing driving strength [9,30]. Off resonance, we might then also expect sideband broadening and splitting with increasing *detuning* ϵ (for fixed Ω) if we were to replace Ω_r with the generalized Rabi frequency $\Omega_r' = \sqrt{\Omega_r^2 + \epsilon^2}$ [9], leading to similar trends for increasing ϵ as for Ω. However, the experiments of Ref. [9] showed a systematic *narrowing* of the Mollow sidebands with increasing detuning, leaving open the question as to why this might be the case.

In fact, off resonance the expressions for the spectrum become significantly more complicated than in the resonant case, and the above simple reasoning does not hold. To illustrate this, in Fig. 2, from top to bottom, we plot the incoherent emission spectrum, extracted sideband splitting, and extracted full width at half maximum ($= \Gamma$) of the Mollow sidebands, calculated from the full phonon theory. In the latter two cases, the spectrum is fitted by a sum of three Lorentzian functions of the form $L(\omega) = 0.5\Gamma/[(\omega - \omega_p)^2 + (0.5\Gamma)^2]$. The left column corresponds to varying the driving frequency on resonance, whereas the right column corresponds to varying the detuning with a fixed driving strength.

As can be seen by the sideband splittings in the middle left plot, increasing the driving strength on resonance does, as expected, cause the sidebands to move apart linearly with Ω. Also, we see in the middle right plot that moving off resonance appears to alter the sideband splitting in exact accordance with the simple procedure of replacing $\Omega_r \to \sqrt{\Omega_r^2 + \epsilon^2}$. The extracted sideband widths in the lower plots, however, reveal something quite different. On resonance, in accordance with $\gamma_{\rm PD} \sim \Omega_r^2$, we see a systematic broadening of the sidebands with increasing driving strength. In contrast, as we move off resonance, we now see a systematic narrowing of the sidebands,

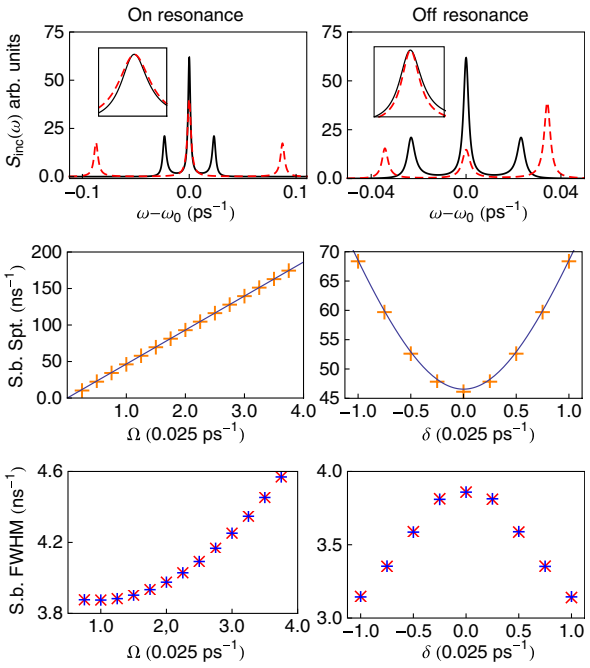

FIG. 2 (color online). From top to bottom, incoherent emission spectrum, extracted sideband splitting, and extracted sideband width for varying driving strength on resonance (left) and varying detuning (right). The solid black curves in the emission spectra are for $\epsilon = 0$, and a driving strength of $\Omega = 0.025$ ps^{-1} (which sets our x-axis units in the rest of the plots). The dashed red curves are for $\Omega = 0.094$ ps^{-1} on resonance, and $\epsilon = \Omega = 0.025$ ps^{-1} off resonance (which has been enhanced by a factor of 5). The insets show the red sidebands shifted and rescaled to lie on top of each other. The solid blue curves in the middle row show the functions $2\Omega_r$ (left) and $2\sqrt{\Omega_r^2 + \epsilon^2}$ (right). The symbols in the bottom row correspond to the red ($\times$) and blue ($+$) sidebands. Parameters: $T_1 = 400$ ps, $\alpha = 0.027$ ps^2, $\omega_c = 2.2$ ps^{-1}, and $T = 10$ K.

consistent with recent experimental results [9]. To further confirm this point, the insets of the plots in the top row show the red sidebands in each case plotted on top of each other. We can gain some approximate analytical insight into this behavior for small detuning by again considering the pure dephasing limit. Allowing for off-resonant driving, we expand the sideband widths to second order in the detuning, from which we find that they are determined by $(3/2)\Gamma_1 + \gamma_{\rm PD} - (\epsilon/\sqrt{2}\Omega_r)^2(\Gamma_1 - 2\gamma_{\rm PD})$. Hence, for $\Gamma_1 > 2\gamma_{\rm PD}$, as in Fig. 2, we expect narrowing as we detune from resonance, whereas broadening occurs for $\Gamma_1 < 2\gamma_{\rm PD}$. Note that while we do not include detailed cavity effects here, which give rise to qualitatively different behavior in Refs. [30,31], our results demonstrate that for a QD TLS at least, an increase in sideband splitting off resonance does not necessarily imply an associated phonon-induced increase in sideband width.

Summary.—We have shown that the balance of coherent to incoherent emission from a driven TLS can be fundamentally altered by environmental interactions, leading to

a nonstandard regime of resonance fluorescence attainable in solid-state emitters. In the context of driven QDs, enhanced coherent scattering can occur with increasing driving strength, due to thermalization in the QD steady state with respect to the phonon bath. This mechanism is in fact rather general and could occur for any emitter in which the steady state becomes dominated by dressed state thermalization. For off-resonant driving, we have shown that QD-phonon interactions do not necessarily lead to broadening in the spectral sideband widths with increasing detuning. In fact, narrowing can occur in certain regimes, consistent with an observed experimental trend [9]. Again, this behavior is not QD specific, and so we expect the emission features outlined above to be of importance in a wide variety of experimental settings.

During the completion of this work we became aware of similar results for the spectral narrowing obtained independently [41]. We thank Stephen Hughes and co-workers for bringing these to our attention. We also thank Clemens Matthiesen, Brendon Lovett, Erik Gauger, and Sean Barrett for fruitful discussions. D. P. S. M. acknowledges support from the EPSRC, CHIST-ERA project SSQN, and CONICET. A. N. is supported by Imperial College.

*daramcc@df.uba.ar
†a.nazir@imperial.ac.uk

[1] B. R. Mollow, Phys. Rev. **188**, 1969 (1969).
[2] H. J. Carmichael, *Statistical Methods in Quantum Optics* (Springer, New York, 1998).
[3] F. Schuda, C. R. Stroud, Jr., and M. Hercher, J. Phys. B **7**, L198 (1974).
[4] X. Xu, B. Sun, P. R. Berman, D. G. Steel, A. S. Bracker, D. Gammon, and L. J. Sham, Science **317**, 929 (2007).
[5] A. Muller, E. B. Flagg, P. Bianucci, X. Y. Wang, D. G. Deppe, W. Ma, J. Zhang, G. J. Salamo, M. Xiao, and C. K. Shih, Phys. Rev. Lett. **99**, 187402 (2007).
[6] S. Ates, S. Ulrich, S. Reitzenstein, A. Löffler, A. Forchel, and P. Michler, Phys. Rev. Lett. **103**, 167402 (2009).
[7] E. B. Flagg, A. Muller, J. W. Robertson, S. Founta, D. G. Deppe, M. Xiao, W. Ma, G. J. Salamo, and C. K. Shih, Nat. Phys. **5**, 203 (2009).
[8] A. N. Vamivakas, Y. Zhao, C.-Y. Lu, and M. Atatüre, Nat. Phys. **5**, 198 (2009).
[9] S. M. Ulrich, S. Ates, S. Reitzenstein, A. Löffler, A. Forchel, and P. Michler, Phys. Rev. Lett. **106**, 247402 (2011).
[10] A. Ulhaq, S. Weiler, S. M. Ulrich, R. Roßbach, M. Jetter, and P. Michler, Nat. Photonics **6**, 238 (2012).
[11] G. Wrigge, I. Gerhardt, J. Hwang, G. Zumofen, and V. Sandoghdar, Nat. Phys. **4**, 60 (2008).
[12] O. Astafiev, A. M. Zagoskin, A. A. Abdumalikov, Yu. A. Pashkin, T. Yamamoto, K. Inomata, Y. Nakamura, and J. S. Tsai, Science **327**, 840 (2010).
[13] A. Zrenner, E. Beham, S. Stufler, F. Findeis, M. Bichler, and G. Abstreiter, Nature (London) **418**, 612 (2002).
[14] A. J. Ramsay, A. V. Gopal, E. M. Gauger, A. Nazir, B. W. Lovett, A. M. Fox, and M. S. Skolnick, Phys. Rev. Lett. **104**, 017402 (2010).
[15] A. J. Ramsay, T. M. Godden, S. J. Boyle, E. M. Gauger, A. Nazir, B. W. Lovett, A. M. Fox, and M. S. Skolnick, Phys. Rev. Lett. **105**, 177402 (2010).
[16] P. Michler *et al.*, Science **290**, 2282 (2000).
[17] C. Santori, M. Pelton, G. Solomon, Y. Dale, and Y. Yamamoto, Phys. Rev. Lett. **86**, 1502 (2001).
[18] C. Santori, D. Fattal, J. Vučković, G. S. Solomon, and Y. Yamamoto, Nature (London) **419**, 594 (2002).
[19] E. B. Flagg, A. Muller, S. V. Polyakov, A. Ling, A. Migdall, and G. S. Solomon, Phys. Rev. Lett. **104**, 137401 (2010).
[20] R. B. Patel, A. J. Bennett, I. Farrer, C. A. Nicoll, D. A. Ritchie, and A. J. Shields, Nat. Photonics **4**, 632 (2010).
[21] H. S. Nguyen, G. Sallen, C. Voisin, Ph. Roussignol, C. Diederichs, and G. Cassabois, Appl. Phys. Lett. **99**, 261904 (2011).
[22] C. Matthiesen, A. N. Vamivakas, and M. Atatüre, Phys. Rev. Lett. **108**, 093602 (2012).
[23] K. Konthasinghe *et al.*, Phys. Rev. B **85**, 235315 (2012).
[24] A. Kiraz, M. Atatüre, and A. Imamoglu, Phys. Rev. A **69**, 032305 (2004).
[25] S. Benjamin, B. Lovett, and J. M. Smith, Laser Photonics Rev. **3**, 556 (2009).
[26] A. Nazir, Phys. Rev. B **78**, 153309 (2008).
[27] P. Machnikowski and L. Jacak, Phys. Rev. B **69**, 193302 (2004).
[28] A. Vagov, M. D. Croitoru, V. M. Axt, T. Kuhn, and F. M. Peeters, Phys. Rev. Lett. **98**, 227403 (2007).
[29] D. P. S. McCutcheon and A. Nazir, New J. Phys. **12**, 113042 (2010).
[30] C. Roy and S. Hughes, Phys. Rev. Lett. **106**, 247403 (2011).
[31] C. Roy and S. Hughes, Phys. Rev. B **85**, 115309 (2012).
[32] K. J. Ahn, J. Förstner, and A. Knorr, Phys. Rev. B **71**, 153309 (2005).
[33] A. Moelbjerg, P. Kaer, M. Lorke, and J. Mork, Phys. Rev. Lett. **108**, 017401 (2012).
[34] E. del Valle and F. P. Laussy, Phys. Rev. Lett. **105**, 233601 (2010).
[35] I. Wilson-Rae and A. Imamoglu, Phys. Rev. B **65**, 235311 (2002).
[36] D. P. S. McCutcheon, N. S. Dattani, E. M. Gauger, B. W. Lovett, and A. Nazir, Phys. Rev. B **84**, 081305(R) (2011).
[37] J. Förstner, C. Weber, J. Danckwerts, and A. Knorr, Phys. Rev. Lett. **91**, 127401 (2003).
[38] A. Krugel, V. M. Axt, T. Kuhn, P. Machnikowski, and A. Vagov, Appl. Phys. B **81**, 897 (2005).
[39] R. Silbey and R. A. Harris, J. Chem. Phys. **80**, 2615 (1984).
[40] See the Supplemental Material at http://link.aps.org/supplemental/10.1103/PhysRevLett.110.217401 for full details of the derivation.
[41] A. Ulhaq, S. Weiler, C. Roy, S. M. Ulrich, M. Jetter, S. Hughes, and P. Michler, Opt. Express **21**, 4382 (2013).